

Role of lattice mismatch and surface chemistry in the formation of epitaxial semiconductor-insulator interfaces

Marjorie A. Olmstead

Department of Physics, University of California, Berkeley, Berkeley, California 94720

R. D. Bringans

Xerox Corporation, Palo Alto Research Center, 3333 Coyote Hill Road, Palo Alto, California 94304

(Received 22 June 1989; revised manuscript received 13 November 1989)

The formation of $\text{SrF}_2/\text{Si}(111)$ and $\text{Ge}/\text{CaF}_2/\text{Si}(111)$ interfaces is studied with photoemission and compared to previous results for the $\text{CaF}_2/\text{Si}(111)$ interface. The interface between SrF_2 and $\text{Si}(111)$ is found to be nonstoichiometric, similar to the interface between CaF_2 and $\text{Si}(111)$: the bonding is between Si and the cation, with a layer of fluorine missing at the interface. In the case of Ge growth on $\text{CaF}_2/\text{Si}(111)$, a variety of effects are noted: The $\text{CaF}_2/\text{Si}(111)$ valence-band offset is reduced by about 1 eV upon deposition of Ge at room temperature. The sticking coefficient of the Ge is significantly increased by preparing the CaF_2 surface with electron bombardment to remove the top layer of fluorine. For both the irradiated and nonirradiated cases, annealing of thin room-temperature-deposited films resulted in Ge island formation.

I. INTRODUCTION

Epitaxial semiconductor-insulator systems, the prototype being $\text{CaF}_2/\text{Si}(111)$, are of both intrinsic scientific interest and technological importance. Scientific interest arises from questions involving interface formation between dissimilar materials: ionic compound insulators, such as CaF_2 and SrF_2 , and the covalent, homopolar semiconductors Si and Ge. Technological interest lies in the development of crystalline dielectrics for use in novel integrated circuits. The growth of the first few monolayers of $\text{CaF}_2/\text{Si}(111)$ has been studied *in situ* with photoemission,¹⁻⁴ soft-x-ray absorption,⁵ and medium-energy ion scattering (MEIS).⁶ Several discussions of the $\text{CaF}_2/\text{Si}(111)$ structure assumed that the CaF_2 molecule remained intact at the interface with a $\text{Si}-(\text{F}-\text{Ca}-\text{F})_n$ layer sequence. However, there is now general agreement that the high-temperature growth interface is not stoichiometric, but rather consists of direct Si—Ca bonds with a dipole moment perpendicular to the interface and no intervening fluorine layer. This means that the CaF_2 molecule is dissociated upon interaction with the $\text{Si}(111)$ substrate. Based on the results of the $\text{CaF}_2/\text{Si}(111)$ system, summarized below, we have extended these studies to include the role of lattice mismatch [$\text{SrF}_2/\text{Si}(111)$] and order of growth [Ge/CaF_2].

Both CaF_2 and Si have face-centered-cubic lattice structures, with either one CaF_2 molecule or two Si atoms as the basis. In the case of $\text{CaF}_2/\text{Si}(111)$, the lattice mismatch between the two crystals is only 0.6% at room temperature or 2.4% at the optimal growth temperature of 700–750 °C (see Table I). This means that the primary constraint determining the equilibrium interface structure for very thin films is the chemical bonding between the two materials, and not structural mismatch. Two possible models consistent with the spectroscopic re-

sults for the fluoride/semiconductor interface are shown in Fig. 1. The experimental results¹⁻⁶ indicate that at the interface there are Si—Ca bonds (with similar charge transfer to that found in CaSi_2), Ca in a 1+ oxidation state, and a 1×1 interface unit cell. This implies that the F layer which would be present at the interface for fully stoichiometric CaF_2 is missing, and that Ca atoms most likely reside in one of the three high-symmetry sites on the $\text{Si}(111)$ surface: directly above the top Si layer (top site), above the second layer Si (T_4 site), or above the fourth layer Si (H_3 site). In thicker films, the CaF_2 overlayer is found to be rotated 180° from the underlying Si substrate, so-called “type-B” epitaxy.⁷ If the Ca were to sit in the H_3 site, this rotation would cause the next F layer to be hindered by the first-layer Si atoms; this structure is thus unlikely to occur. The photoemission¹⁻⁴ and x-ray-absorption⁵ results cannot distinguish between the other two high-symmetry sites, and these two possible structures are shown in Fig. 1. The T_4 site (right) is indicated by MEIS results for a single monolayer of Ca and F on the $\text{Si}(111)$ surface;⁶ the top site (left) is favored by some transmission electron microscopy results,⁸ but not by others,⁹ while still another group finds two structures simultaneously.¹⁰

The $\text{CaF}_2/\text{Si}(111)$ interface has been studied theoretically by Satpathy and Martin.¹¹ The total energy of the $\text{CaF}_2/\text{Si}(111)$ interface is found to be the lowest for an interface in which there are two F layers separating the Si and Ca layers; however, in the absence of excess fluorine, interfaces such as those shown in Fig. 1 without F at the interface are found to be stable. The T_4 structure shown in Fig. 1 has the lowest total energy of the four F deficient models tested by Satpathy and Martin, although the energy differences were small enough that further relaxation may change the ordering. The stoichiometric interface, on the other hand, is not stable with respect ei-

TABLE I. Semiconductor and fluoride materials parameters. Lattice constants at room temperature (Ref. 34) and growth temperature (Ref. 35) and their ratios to those of the Si substrate; energy gaps and surface free energy (Ref. 36).

Material	Lattice constant		Lattice constant		Energy gap (eV)	Surface energy (erg/cm ²)
	298 K (nm)	Ratio to Si	1005 K (nm)	Ratio to Si		
Si	0.5431	1.000	0.5440	1.000	1.1	1240 (Refs. 37 and 38)
Ge	0.5657	1.042	0.5684	1.045	0.7	1060 (Ref. 38)
CaF ₂	0.5463	1.006	0.5571	1.024	12.1	450 (Ref. 37)
SrF ₂	0.5799	1.068	0.5880	1.081	11.3	360 (Ref. 39)
BaF ₂	0.6200	1.142	0.6305	1.159	11.0	280 (Ref. 37)

ther to bulk materials plus surfaces or to disproportionation into the F-rich and F-deficient structures. The valence-band offset is also a strong function of the F concentration at the interface due to the interface dipole created by charge transfer between the Si and CaF₂. There is an uncertainty in comparison with experiment due both to the inherent problems of the local-density approximation and to the difference in the experimental and theoretical definitions of band offsets. However, on the basis of comparing the experimental band offset and the total energy, Satpathy and Martin concluded that the two models in Fig. 1 were the most likely to explain the type-B interface, with the directional bonding (left) having the more appropriate band offset and the silicide bonding (right) having the lower total energy.¹¹

Strontium fluoride is chemically very similar to calcium fluoride, but its lattice constant is significantly larger. The Si-SrF₂ lattice mismatch is 6.8% at room temperature and 8.1% at the growth temperature (see Table I). It has been shown with transmission electron microscopy that the BaF₂/Ge(111) interface, with a mismatch of 9.6% (10.9%) at room (growth) temperature exhibits a “discommensurate” interface, where orientational order is maintained across the interface, but each material maintains its bulk lattice constant.¹² The SrF₂/Si(111) system is intermediate between these two cases, and the question arises as to whether the strong Si-cation bonding observed at the CaF₂/Si(111) interface will be maintained at the SrF₂/Si(111) interface. We present here a comparative photoemission study of the CaF₂/Si(111) and SrF₂/Si(111) interfaces. We find the chemical bonding and charge transfer at the interface to be very similar in both cases, with covalent Si—Ca and Si—Sr bonding at the respective interfaces.¹³

The nonstoichiometric interface we have found for both the CaF₂/Si(111) and SrF₂/Si(111) systems has important implications for the inverse growth of Si or Ge on top of these fluorides. Photoemission experiments of solid-phase epitaxy after room-temperature deposition of CaF₂/Si(111) (Ref. 2) and of electron irradiation of CaF₂/Si(111) grown at 500 °C (Ref. 4) show that high temperatures or some other perturbation such as high-energy electrons are required to dissociate the CaF₂ molecule at the interface. The natural termination of

CaF₂(111), however, is a complete F—Ca—F triple layer. On the basis of these results, we predicted that the growth of Si and related materials on CaF₂ would be enhanced by the removal of the top fluorine layer.⁴ This has been confirmed for thick layers of Ge (Ref. 14) and GaAs (Ref. 15) on CaF₂/Si(111), where the morphology of the semiconductor overlayer was markedly improved by electron irradiation. In this work, we present photoemission results for the initiation of Ge growth on CaF₂/Si(111) both on irradiated and nonirradiated substrates.¹⁶ We find that the sticking coefficient and wetting of the Ge overlayer increases with irradiation. We also find that the deposition of Ge on thin CaF₂/Si(111) films reduces the Si—CaF₂ valence-band offset by about 1 eV, similar to what was observed for Au/CaF₂/Si(111).¹⁷

II. EXPERIMENTAL CONSIDERATIONS

Calcium fluoride and strontium fluoride were grown on Si(111) (*p* type, $\rho=0.01 \Omega \text{ cm}$) by molecular-beam epitaxy at substrate temperatures of $710 \pm 20^\circ \text{C}$, as measured by an optical pyrometer. In one case, a SrF₂ film was grown on a substrate not intentionally heated ($T_{\text{sub}} \sim 50^\circ \text{C}$ due to radiation from the 1300 °C SrF₂ Knudsen cell). The

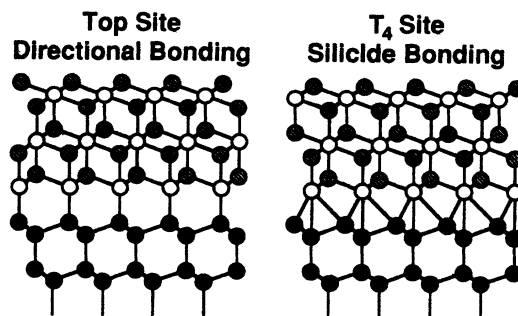


FIG. 1. Model structures for the CaF₂/Si(111) or SrF₂/Si(111) interface which are consistent with spectroscopic and theoretical results. Current results cannot distinguish between the directional bonding with the cation in the “on-top” site (left) and silicide bonding with the cation in the “T₄” site (right). Hatched circles, fluorine; open circles, calcium or strontium; solid circles, silicon.

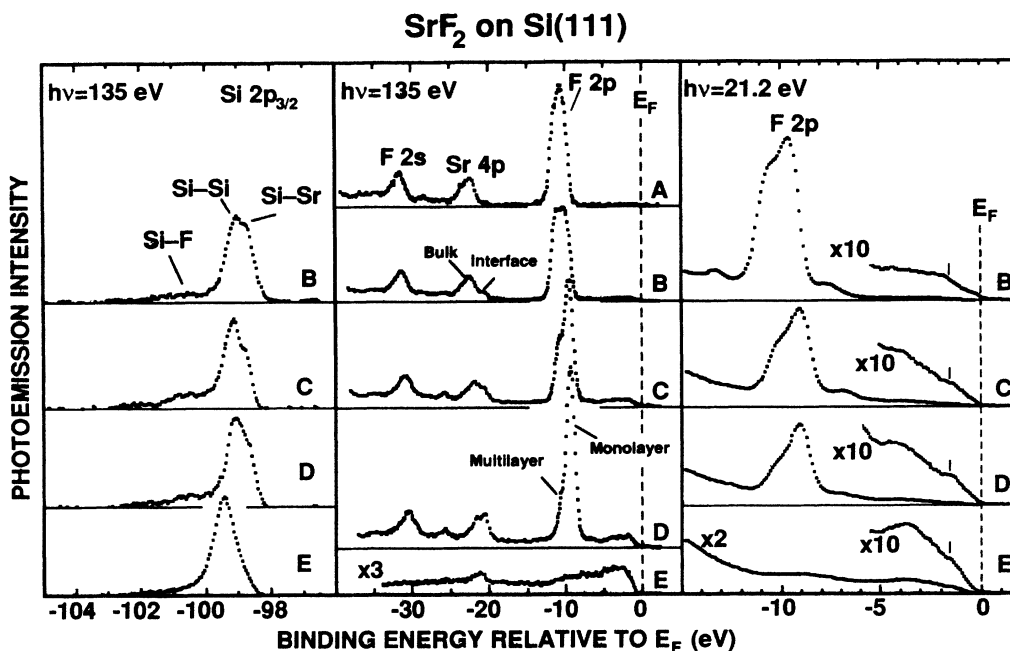


FIG. 2. Comparison of photoemission spectra for $\text{SrF}_2/\text{Si}(111)$, *A*: > 1.5 -nm film, $T_{\text{sub}} \sim 50^\circ\text{C}$, *B*: 1.1-nm film, $T_{\text{sub}} = 700^\circ\text{C}$, 75-s growth, *C*: 0.6-nm film, $T_{\text{sub}} = 710^\circ\text{C}$, 30-s growth, *D*: 1 min, 750°C anneal of film *C*. *E*: 1 min, 800°C anneal of film *D*. Left panel: $\text{Si } 2p_{3/2}$, $h\nu = 135$ eV. Center panel: shallow core levels, $h\nu = 135$ eV. Right panel: valence bands, $h\nu = 21.2$ eV.

substrates were prepared by growing a thin oxide film¹⁸ prior to their introduction into the vacuum chamber. Clean surfaces were then obtained by sputtering (500-eV Ar^+ ions) and annealing. The samples were heated by passing a direct current through them. The film deposition was carried out in a separate growth chamber connected by a transfer chamber to the main analysis chamber. All three chambers had a base pressure in the 10^{-10} Torr range.

For the growth of Ge on CaF_2 , thin (~ 1.2 nm) CaF_2 films were first grown at 700°C on $\text{Si}(111)$ and characterized. Ge was then evaporated onto these unheated substrates. Electron irradiation of the pristine CaF_2 film was performed at room temperature on ~ 10 mm² of the sample by moving the sample beneath a normal incidence beam of 3-keV electrons (0.8 μA with a spot diameter of 1.5 mm). The total exposure in the central region was 2.2×10^{-4} C/cm², or about two electrons per unit cell.

Core-level photoemission spectra were obtained using synchrotron radiation at the Stanford Synchrotron Radiation Laboratory (Stanford, CA). No evidence of radiation damage due to the synchrotron beam was observed for the photon energies used ($h\nu = 109$ – 112 , 135, and 387 eV). Valence-band photoemission spectra were obtained using a HeI discharge lamp ($h\nu = 21.2$ eV). A cylindrical-mirror analyzer was used to collect the photoemitted electrons. The axis of the analyzer was 75° from the incident photon beam and 10° from the sample normal for the synchrotron measurements; it was 95° from the incident light and 38° from the sample normal for the discharge-lamp measurements. The position of the Fermi level was determined via emission from a gold foil in electrical contact with the sample holder.

III. RESULTS AND DISCUSSIONS

A. $\text{SrF}_2/\text{Si}(111)$

1. Shallow core levels

The shallow core levels for a variety of $\text{SrF}_2/\text{Si}(111)$ films and treatments are shown in the center panel of Fig. 2. For the top spectrum, *A*, a “thick” (≥ 1.5 nm) film was grown on an unheated substrate (90 s growth). The three features observed arise from the $\text{F } 2p$, $\text{Sr } 4p$, and $\text{F } 2s$ atomic levels. The $\text{F } 2p$ states form the SrF_2 valence band; the $\text{Sr } 4p$ line shape is consistent with a spin-orbit splitting of 1.2 eV and the statistical ratio of 1:2. For the thick film, the $\text{Sr } 4p$ peak is predominantly due to Sr^{2+} ions in the bulk lattice.

Photoemission spectra from a $\text{SrF}_2/\text{Si}(111)$ film about three triple layers (1.1 nm) thick (75 sec growth at a bulk rate of $10 \text{ \AA}/\text{sec}$, $T_{\text{sub}} = 700^\circ\text{C}$) are shown as spectra *B* in Fig. 2. The $\text{Sr } 4p$ level (see also Fig. 3) clearly shows an additional peak shifted to lower binding energy from the bulk peak, similar to that seen for the $\text{Ca } 3p$ (Fig. 4) and $\text{Ca } 2p$ (Fig. 5) levels at the $\text{CaF}_2/\text{Si}(111)$ interface. The low binding energy Ca peak has been attributed to Ca bonded to Si in a 1+ oxidation state at the interface.^{1–5} Figure 2 depicts spectra *C* from a film 1.5–2 triple layers thick (30 sec growth at 710°C), and spectra *D* in Fig. 2 were taken on the same film after a 1 min anneal at 750°C which resulted in a partial reevaporation of the film. The small peak at about -25.5 eV in spectra *C* and *D* is due to a slight Ca contamination.¹⁹ After a further 1 min anneal at 800°C , the fluorine is all gone and a small amount of Sr remains on the $\text{Si}(111)$ surface (spectra *E* in Fig. 2).

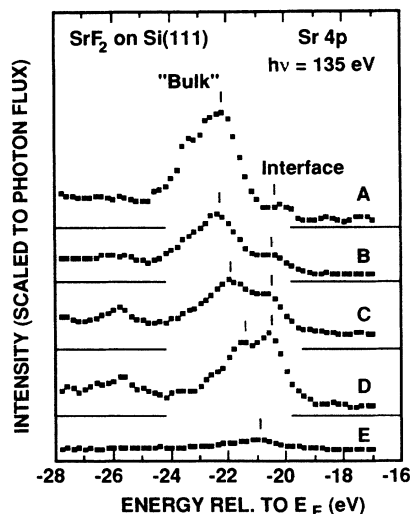


FIG. 3. Comparison of Sr 4*p* spectra for SrF₂/Si(111). *A*: > 1.5-nm film, $T_{\text{sub}} \sim 50^\circ\text{C}$. *B*: 1.1-nm film, $T_{\text{sub}} = 700^\circ\text{C}$, 75-s growth. *C*: 0.6-nm film, $T_{\text{sub}} = 710^\circ\text{C}$, 30-s growth. *D*: 1 min, 750°C anneal of film *C*. *E*: 1 min, 800°C anneal of film *D*. Spectra are normalized to photon flux.

The low-energy diffraction (LEED) pattern for this surface was a fuzzy 4×1 . Different annealing conditions result in a variety of LEED patterns, including 2×1 and 5×1 , depending on coverage. This is similar to the 2×1 , 3×1 , and 5×1 patterns observed after similar annealing of the CaF₂/Si(111) system.^{3,4}

The low-binding-energy component of the Sr 4*p* peak is indicative of Sr—Si bonding at the interface, similar to the case of CaF₂/Si(111). This is the peaked labeled “interface” in the center panel of Fig. 2 and in Fig. 3. For the three thin, high-growth-temperature films (*B*, *C*, and *D*), fitting the Sr 4*p* peak to either two or three spin-orbit pairs (to account for the variation in the “bulk” contribution) always results in a peak at a binding energy of

20.52 ± 0.05 (relative error) ± 0.05 (absolute error) eV below the Fermi level, and the intensity of this peak was independent of the fitting procedure (within 2%). The ratio of the intensity in the component at 20.5 eV to the total emission is 0.20, 0.50, and 0.69 (± 0.01) for films *B*, *C*, and *D*, respectively.

The identification of the low-energy Sr 4*p* peak as being due to the interface is confirmed by its increase in magnitude relative to the bulk peak, and its constancy in position relative to the Si 2*p* state in thinner films. Assuming laminar growth and an electron escape depth in SrF₂ of 1.1 nm (Ref. 20) (intensity loss of 25% with each layer), the film thicknesses calculated from the intensity ratios are 3.5, 1.8, and 1.4 triple layers for films *B*, *C*, and *D*, respectively. These values are consistent with the preparation conditions if we assume that more reevaporation took place during the longer growth of film *B* or a smaller sticking coefficient for successive layers than for the first. Calibration of the same Knudsen cell in a different vacuum system, but with similar geometry, gave a growth rate of 10 ± 1 Å/min on a room-temperature substrate, or 3.7 ± 0.4 ml for a 75 sec growth. The Sr 4*p* peak for the Si(111):Sr surface (spectrum *E*) has a binding energy relative to the Fermi level which is 0.4 higher than the interface peak. However, the energy relative to the Si 2*p* level (left-hand panel of Fig. 2) is the same for both the SrF₂/Si(111) interface and the Si(111):Sr surface, indicating similar bonding and charge transfer, but a Fermi-level pinning position closer to the middle of the Si band gap for the latter case.

While the energy of the interface contribution remains the same relative to the Si 2*p* level in the various films, the “bulk” peak (marked with a tick in Fig. 3) shifts to lower binding energy and changes shape with decreasing thickness. We discuss three possible explanations. One is that this shallow core state is broadened into a band which changes shape as the film gets thinner. A second is the existence of a surface contribution at an energy intermediate between the bulk and interface state. If this is

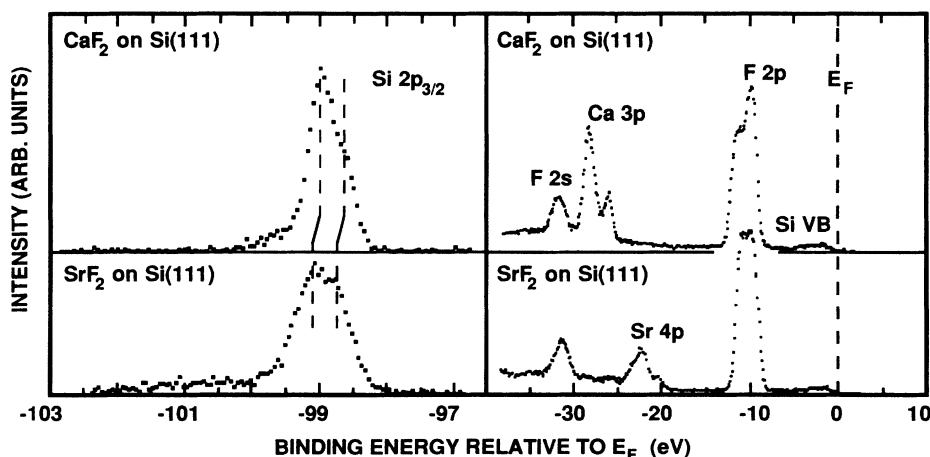


FIG. 4. Comparison of CaF₂/Si(111) (top) and SrF₂/Si(111) (bottom) spectra for 1.1-nm-thick films grown at 700°C . All spectra were taken at 135 eV except for the Si 2*p* at the CaF₂/Si(111) interface, which was taken at 130 eV (the 130-eV spectrum has better resolution and less interface sensitivity).

the case, then the relative intensities of the bulk, surface, and interface components indicate a nonlaminar-growth mode (the third layer starting before the first layer is completed). A third possibility is a change in screening as the Sr ions are increasingly influenced by the high dielectric constant of the Si in thinner films. This is likely the cause² of the 1-eV shift of the F 2s level with film thickness, which is apparent in Fig. 2. It is likely that the dominant effect on the Sr 4p emission is the modification of the band structure with thickness (leading to the change in shape of the peak), combined with a small overall shift due to screening. It should be noted that these effects are coupled, with altered screening affecting the band structure. While calculations for SrF₂ 4p states are not available, the equivalent highest-occupied cation states for both CaF₂ and CdF₂ show a weak dispersion.²¹ The energy positions of the noninterface peaks are not constant among the different films, and in particular there is no clear surface contribution to spectrum *A* in Fig. 2, making the separate-surface-component explanation unlikely. The energy shifts do not uniformly parallel the shift in the F 2s state, implying that more than just screening is involved.

The F 2p-state emission becomes more asymmetric as the film thins. This can be attributed both to changing band structure and to the contribution (labeled "Monolayer" in Fig. 2) of an uncovered interface layer. The F 2p band arises from the overlap of the various F 2p orbitals in the bulk fluoride. The Sr 4p and Si 2p (see below) results indicate that the bonding is directly between the Sr and Si atoms, and that the interface is nonstoichiometric. When just a single layer of SrF₂ is on the surface, each unit cell then consists of one Sr and only one F atom, as was seen⁶ for the CaF₂/Si(111) case. The narrow peak is thus due to the single, uncovered F layer. The fractional intensity of the low-energy F 2p peak is consistent with the thicknesses inferred from the Sr-interface peak intensity.

An additional datum to be obtained from Fig. 2 is the valence-band offset at the SrF₂/Si(111) interface. Extrapolating the tops of the valence bands with straight lines, one obtains an offset of 8.2 eV, within the range of values found for similarly prepared CaF₂/Si(111) interfaces (see Fig. 6). The results of Satpathy and Martin¹¹ show that the band offset is a function of the interface dipole, which is turn dependent on the F concentration (and hence interface charge) and the distance over which charge is transferred. The similarity in the CaF₂ and SrF₂ results indicates similar bonding and similar interface states in the two cases.

A comparison of the shallow core levels and Si 2p_{3/2} emission for SrF₂/Si(111) and CaF₂/Si(111) is shown in Fig. 4. The SrF₂/Si(111) spectra are from film *B* and the CaF₂/Si(111) spectra were obtained under similar growth conditions.⁴ The similarities in the two sets of spectra which were discussed above can clearly be seen in the figure.

2. Substrate core level

The Sr and F spectra in Fig. 2 indicate that the Sr binding energy is modified at the interface, that the F 2s

levels shift to lower binding energy and broaden as the film is thinner, and that the F 2p band structure only develops after the deposition of the second molecular layer. It is not possible to tell whether both Sr and F are bonded to Si from the shallow core levels alone. Rather, one must investigate the Si core level. The left-hand panel of Fig. 2 shows the Si 2p_{3/2} emission from the same films as the shallow core-level spectra (except for film *A* where the Si 2p was barely visible). The data are shown after (quadratic) background subtraction and spin-orbit deconvolution. The deconvolution requires no curve fitting, but is a numerical manipulation of the spectra, having only the spin-orbit splitting (0.605 eV) and the spin-orbit ratio (assumed to be the statistical value of 1:2) as inputs. Assuming that the bulk Si 2p_{3/2} peak is 98.82 eV from the valence-band maximum,²² the Fermi level is approximately 0.2 eV above the Si valence-band maximum, similar to the case¹⁻⁴ for CaF₂/Si(111) (see Fig. 4).

The principal contributions to the Si 2p peak for all four spectra in Fig. 2 are the bulk contribution (measured in a bulk-sensitive spectrum to be at -99.03 ± 0.05 eV for film *B*) and a contribution from the interface, which is shifted to lower binding energy. This interface component has a binding energy 0.35–0.40 eV less than that for bulk Si, consistent with Si–Sr bonding. The measured shift for Si–Ca bonding at the CaF₂/Si(111) interface is 0.36 eV.⁴ The Pauling electronegativities are the same for Sr and Ca, so the similarity in binding energy shifts indicates that the charge transfer and bonding is similar in the two cases.

There is also some Si 2p_{3/2} intensity shifted to higher binding energy from the bulk Si peak. This is indicative of either Si–F bonding or Si dangling bonds at the interface. Also, a small contribution at high binding energy (low kinetic energy) can result from inelastic scattering of the electrons from the peak as they go through a disordered overlayer. The chemical shift for a monolayer of F on Si(111) is 1.0 eV to higher binding energy.²³ This indicates that some of the Si atoms at the SrF₂/Si(111) interface may be bonded to more than one F atom, implying that a small fraction of the interface contains defects on the Si side of the interface. There is also some intensity at an energy about 0.6–0.8 eV from the Si bulk peak, indicative of Si–F bonds with less charge transfer. The dominant contribution due to dangling bonds on the Si(111)-(7×7) surface is found to be in the range of 0.3–0.7 eV to higher binding energy from the bulk peak,²⁴ with a smaller contribution at lower binding energy than the bulk. For spectrum *E*, there is no fluorine and only a small amount of Sr ($\lesssim \frac{1}{4}$ ml) on the surface (see center and right panels), so that the high-binding-energy tail must be due to uncovered Si atoms. The asymmetry on the low-binding-energy side of spectrum *E* arises primarily from the Si atoms bonded to Sr.

The fraction of the interface with Si–F bonding is largest for the sample whose spectrum is shown in *C* of Fig. 2. This sample spent the shortest time at high temperature after the deposition of the first SrF₂ layer. The intensity of the Si–Sr component increases at the expense of the Si–F components when this sample is annealed for 1 min at 750 °C (spectra *D* in Fig. 2). This supports the

hypotheses that the SrF_2 molecule must dissociate at the interface to form the low-energy interfacial structure involving Si—Sr bonds and that this dissociation is a thermally activated process. This has also been proposed for the $\text{CaF}_2/\text{Si}(111)$ system.^{2,4} The narrow temperature window for obtaining a uniform Si—Sr bonded interface begins near the temperature where the 7×7 reconstruction begins to disorder on the clean surface. The upper edge of the window for growth lies at the reevaporation temperature for the overlayer. This is similar to many epitaxial-growth situations; the optimal growth temperature is just below the reevaporation temperature, so that if a molecule does not diffuse into the deepest energy well it will not stick.

3. Valence bands

If there is direct Si—Sr bonding at the $\text{SrF}_2/\text{Si}(111)$ interface, then the occupied bonding level should be observable in ultraviolet photoemission spectroscopy. Spectra obtained using 21.2-eV HeI photons for the same films as the shallow core levels and Si $2p_{3/2}$ are shown in the right-hand panel of Fig. 2. We attribute the shoulder at 1.7 eV below the Fermi level (marked with a tick) to this interface state. Its intensity is maximum for film *D*, the thinnest film for which there is still a full monolayer of Si—Sr bonds, and it is still present for the $\text{Si}(111):\text{Sr}$ surface where there is less than a full monolayer of Sr and no F atoms. A similar state which disperses from 0.75 eV below E_{VBM} at the $\bar{\Gamma}$ point of the surface Brillouin zone to 1.4 eV at the \bar{M} point has been observed at the $\text{CaF}_2/\text{Si}(111)$ interface.²³ Due to the large density of states at the surface Brillouin-zone boundary, the position of the peak in an angle-integrated photoemission measurement of $\text{CaF}_2/\text{Si}(111)$ is expected to be 1.3 eV below E_{VBM} or about 0.2 eV higher than the observed position in Fig. 2 for $\text{SrF}_2/\text{Si}(111)$. This similarity between the results again supports the thesis that the bonding is very similar at the $\text{SrF}_2/\text{Si}(111)$ interface to that at the $\text{CaF}_2/\text{Si}(111)$ interface. This state has been studied with tight-binding calculations for the $\text{CaF}_2/\text{Si}(111)$ interface,²⁵ and is derived from the interaction of the Si $3p$ with the Ca $4s$ and $4p$. The small difference in interface state energy may be due to the smaller band gap of SrF_2 , placing the Sr $5s$ level closer to the Si valence band.

The results described above the $\text{SrF}_2/\text{Si}(111)$ interface demonstrate that the principal interfacial bonding is dominated by chemical driving forces and not by the strain induced by lattice mismatch. There is more disorder and scattering at the interface with the large lattice mismatch, and these results do not tell us if the interface is pseudomorphic, but they do tell us that the choice of which atoms will bond is not affected by the lattice mismatch and is the same for the $\text{CaF}_2/\text{Si}(111)$ and $\text{SrF}_2/\text{Si}(111)$ interfaces. Low-energy electron diffraction studies of samples grown under similar conditions show that the first monolayer is constrained by the silicon lattice constant, but that the SrF_2 jumps to nearly its own lattice constant upon initiation of the second layer, at least in the lateral dimension.²⁶ The results for $\text{SrF}_2/\text{Si}(111)$ imply that we can learn about interface

bonding in the inverted case of semiconductor/fluoride without being forced to rely on lattice matching.

B. Ge/ $\text{CaF}_2/\text{Si}(111)$

We have studied the system of $\text{Ge}/\text{CaF}_2/\text{Si}(111)$, where the starting $\text{CaF}_2/\text{Si}(111)$ structure is similar to that whose spectra are shown in Fig. 4. A thin layer of Ge was then deposited at room temperature on this starting structure and subsequently annealed. The use of thin CaF_2 and Ge layers and the different semiconductor elements for the substrate (Si) and overlayer (Ge) allows monitoring of the substrate Si $2p$ core level for any changes at the buried interface.

The alkaline-earth fluorides CaF_2 and SrF_2 grow in a laminar fashion on $\text{Si}(111)$ surface. A primary reason for this layer-by-layer growth is that the surface free energy (as determined by cleavage energies) of the fluorides is significantly less than that of the Si substrate (see Table I). For the inverse process of semiconductor growth on the fluorides, the natural growth mode would be island formation, due to the lower surface free energy of the substrate. The growth of an overlayer island results in the replacement of the area of exposed substrate by equal areas of interface and exposed overlayer. In order for the total energy to favor laminar growth, it is necessary for the interface energy to be less than the difference in surface energies:

$$\gamma_{SO} < \gamma_{SV} - \gamma_{OV} ,$$

where γ_{ij} denotes the interface energy per unit area for the *ij* interface, *S* denotes the substrate, *V* the vacuum and *O* the overlayer. Thus to promote the growth of Si or Ge on CaF_2 , it is desirable both to increase the surface energy of the CaF_2 substrate and to decrease the energy of the formed interface. The results discussed above indicate that removing the surface fluorine layer from the $\text{CaF}_2(111)$ surface should accomplish both of these goals. If the natural (111) cleavage termination is between the F layers, then the Ca terminated surface must have a higher surface energy. Similarly, if the equilibrium interface for the growth of CaF_2 on Si involves the removal of the interface F layer, it is expected that the removal of this layer from the CaF_2 substrate will lower the interface energy during growth of Si or Ge on CaF_2 . We have removed the surface F layer by electron irradiation²⁷ in one portion of the $\text{CaF}_2/\text{Si}(111)$ substrate to allow a comparison of the growth of Ge on $\text{CaF}_2/\text{Si}(111)$. First, however, we will discuss the growth of Ge on a nonirradiated $\text{CaF}_2/\text{Si}(111)$ substrate.

1. Ge deposition on nonirradiated $\text{CaF}_2/\text{Si}(111)$

Photoemission spectra for a particular case of a $\text{Ge}/\text{CaF}_2/\text{Si}(111)$ growth are shown in Fig. 5. The relative amplitudes of the Si $2p$, Ca $2p$, and shallow core levels are arbitrary, but within each level the spectra are shown normalized to the incident photon flux on the sample.²⁸ The bottom set of spectra was taken from the pristine $\text{CaF}_2/\text{Si}(111)$ film. From comparison with our previous results, we estimate the CaF_2 film to be about 1.2 nm

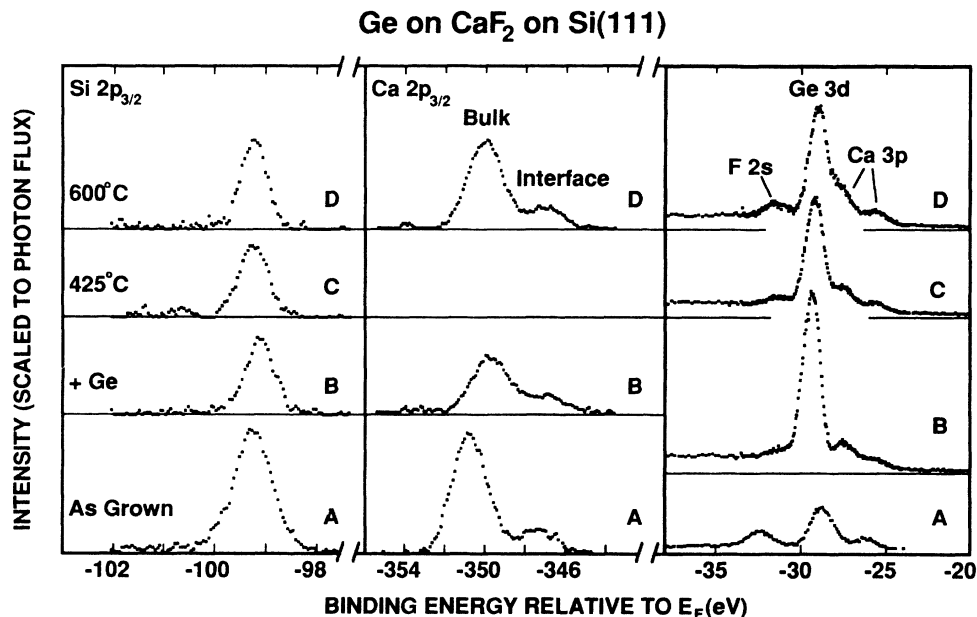


FIG. 5. Photoemission spectra for Ge/CaF₂/Si(111). *A*: As-deposited CaF₂/Si(111). *B*: After deposition of 0.45-nm Ge at room temperature on film *A*. *C*: 1 min, 425°C anneal of film *B*. *D*: 1 min, 600°C anneal of film *C*. Left panel: Si 2p_{3/2}, $h\nu=135$ eV (the resolution for these spectra is a factor of 4 less than for the Si 2p spectra in Figs. 2 and 4). Center panel: Ca 2p_{3/2}, $h\nu=387$ eV (after background subtraction and spin-orbit deconvolution). Right panel: F 2s, Ge 3d and Ca 3p, $h\nu=135$ eV (raw data).

thick. The subsequent spectra, *B* in Fig. 5, were taken after the deposition of Ge onto the CaF₂/Si(111) film at room temperature. The Si 2p [kinetic energy (KE) of ~ 30 eV], Ca 2p (KE of ~ 30 eV), and F 2p (KE of ~ 115 eV) (not shown) emission intensities are all reduced by about half, indicating a Ge overgrowth of 0.7 electron escape depths, or about 0.40–0.45 nm (~ 3 ML).²⁹ This thickness estimate assumes uniform coverage of the Ge at room temperature, which may not be true, as the difference in sticking coefficient between the unirradiated fluoride and the Ge could lead to islanding during growth, even at room temperature. At least half of the surface must be covered to account for the 50% reduction in intensity. In that case, the Ge would be more than three or four escape depths thick (~ 15 nm, or 2–3 nm) over one half of the sample. In the case of Si on CaF₂, however, which has a larger free-energy difference than the Ge/CaF₂ case, the deposition 4 nm of Si at room-temperature is known to form a uniform amorphous layer.³⁰ The spectra in *C* and *D* in Fig. 5 were taken after anneals of the Ge/CaF₂/Si(111) system at 425 and 600°C, respectively.

The Si 2p core level is changed very little by the deposition of Ge, indicating that the bonding at the buried interface is unchanged and the Fermi-level pinning position in the Si band gap is not affected to within ± 0.2 eV. The CaF₂ emission, on the other hand, is shifted to lower binding energies by about 1 eV relative to the Fermi level, indicating that $E_F - E_{VBM}$ has changed significantly for the calcium fluoride due to the deposition of Ge. This is seen most clearly in the Ca 2p spectra in Fig. 5, and is summarized for different growths in Fig. 6. This means that the

band offset at the buried CaF₂/Si(111) interface has been changed by about 1 eV due to the deposition of three layers of Ge on top of the CaF₂, several angstroms away from the interface. This shift is relatively independent of the starting band offset at the CaF₂/Si(111) interface. For the three different examples of Ge deposition on nonirradiated CaF₂/Si(111) described in Fig. 6, the starting CaF₂/Si band offsets vary by 0.5 eV, and all three are

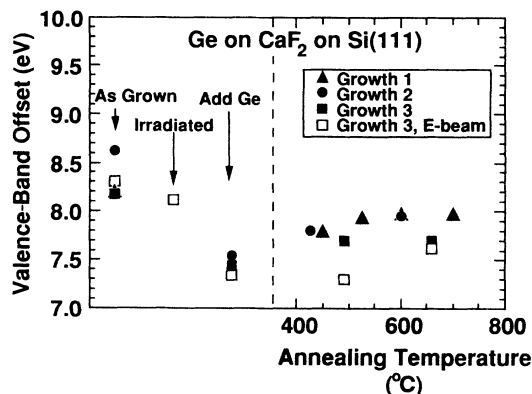


FIG. 6. Si-CaF₂ valence-band offset as a function of Ge deposition at room temperature and subsequent annealing. Growth 1: 0.9-nm Ge. Growth 2: 0.45-nm Ge (from Fig. 5). Growth 3: same sample as Fig. 8 including irradiated and nonirradiated portions of sample. The relative valence-band positions were monitored via the separation between the bulk Si 2p_{3/2} and the Ca 3p peaks, with a separation of 71.2 eV corresponding to a valence-band offset of 8.0 eV.

reduced by about 1 eV upon Ge deposition. The reduction also occurs for the irradiated sample. Upon annealing the offset relaxes back, but is still less than that for uncovered $\text{CaF}_2/\text{Si}(111)$. This behavior is similar to that recently reported for the deposition of gold overlayers on $\text{CaF}_2/\text{Si}(111)$.¹⁷

The Ge $3d$, F $2s$, and Ca $3p$ peaks can be seen in the right panel of Fig. 5. Assuming the bulk separation between the Ge $3d_{5/2}$ and the Ge valence-band maximum³¹ places the Fermi level 0.3 eV below the Ge valence-band maximum for spectrum *B* in the figure. It is unlikely, however, that the Fermi level is pinned below the top of the Ge layer valence states. The Ge is, however, amorphous and only three monolayers thick, so that it is not surprising that the separation between core states, which may be chemically shifted at an interface or surface, and the modified valence states would be different from the bulk value. The Fermi level is pinned near the Si valence-band maximum at the $\text{CaF}_2/\text{Si}(111)$ interface, and the results are consistent with the Fermi level being similarly pinned near the Ge valence-band maximum at the Ge/ CaF_2 interface. If the intrinsic semiconductor-insulator band offset is different by an electron volt for Si- CaF_2 and CaF_2 -Ge, while the Fermi level is pinned at both semiconductor valence-band maxima, then an electric field of about 10^7 V/cm would be developed across the CaF_2 film.

With only four Ca layers, a large electric field across the film would lead to a Ca $2p$ spectrum consisting of a superposition of four peaks at different energies, resulting in a broadening of the peak; similarly, the Ca $3p$, F $2s$, and F $2p$ should also broaden. However, the bulk fluoride peaks do not broaden significantly when Ge is deposited, but rather shift uniformly to lower binding energy, as was seen for Au deposition.¹⁷ The Ca $2p$ interface peak indicated in Fig. 5 broadens somewhat but does not shift significantly, staying constant relative to the Si $2p$. This can be explained if a dipole field is maintained

between the Ca atom nearest the Si substrate and the first bulk layer of CaF_2 instead of developing an electric field across the entire CaF_2 layer.¹⁷ The broadening of the Ca $2p$ interface peak could be due either to a local variation in interface dipole or to Ge—Ca bonding at the top interface contributing at energies intermediate to the bulk and Si—Ca contributions. The similarity between the deposition of a semiconductor and a metal at room temperature on the $\text{CaF}_2/\text{Si}(111)$ structure is not surprising, since the same mechanisms which give rise to the Schottky barrier at an insulator/metal interface are involved in determining the band offset at an insulator/semiconductor interface.

The variation in the $\text{CaF}_2/\text{Si}(111)$ band offset has been correlated with the amount of F at the interface, with a larger band offset for lesser amounts of F.¹¹ Electron irradiation of a F-rich interface has been shown to increase the band offset, as has growth at a higher temperature, where the dissociation of the CaF_2 molecule is more efficient.^{2,4} The action of the Ge, then, is to increase the electron transfer from the CaF_2 -Si interface layer to the bulk CaF_2 , as would occur in the presence of F. The activation energy for ionic conduction in CaF_2 is 1.0 eV,³² so it is likely that a 1-eV drop over four atomic layers would induce some flow of F ions.

Of further interest is the behavior of the Ge/ $\text{CaF}_2/\text{Si}(111)$ system upon annealing. The decreased intensity of the Ge $3d$ relative to the Ca $3p$ and F $2s$ peaks upon annealing can be seen in Fig. 5, as can the increase in the absolute intensity of the Ca $2p$. After the final anneal (600°C), the Ca and F emission intensities are consistent with an effective thickness of only 0.18 nm of Ge, as opposed to the initial 0.45 nm [using an electron escape depth of 0.6 nm (Ref. 29)]. The temperature is too low for significant evaporation of Ge, so these results can only be explained if the Ge has condensed into islands. The tendency to form islands was expected from the surface-energy arguments discussed above, since the Ge

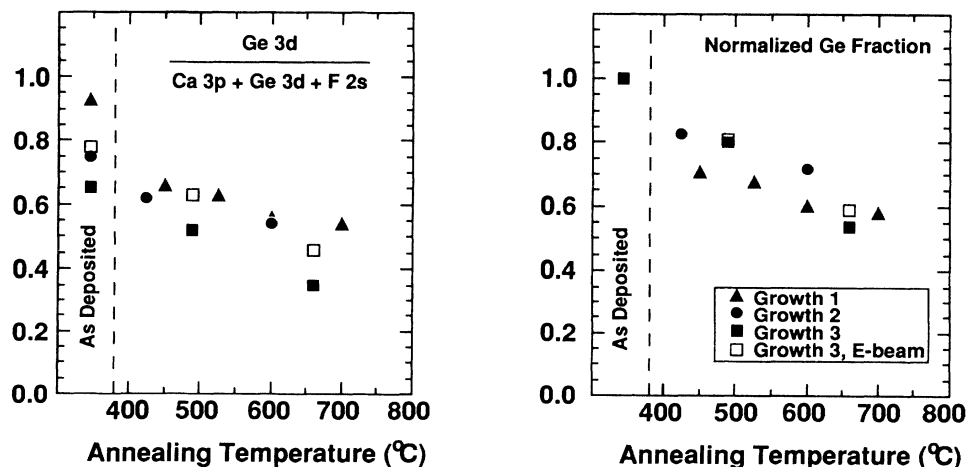


FIG. 7. *A*: Fraction of intensity in combined F $2s$, Ge $3d$, and Ca $3p$ spectrum ($h\nu = 135$ eV) which is due to Ge $3d$ emission. *B*: Data in *A* normalized to the initial value. Growth 1: 0.9-nm Ge. Growth 2: 0.45-nm Ge (from Fig. 4). Growth 3: same sample as Fig. 8 including irradiated and nonirradiated portions of sample.

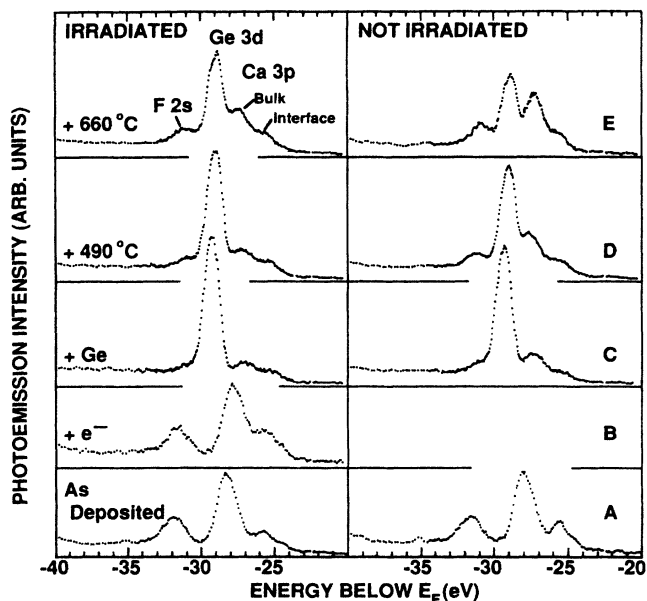


FIG. 8. F 2s, Ge 3d, and Ca 3p for Ge on irradiated (left panel) and nonirradiated (right panel) $\text{CaF}_2/\text{Si}(111)$. A: As-deposited $\text{CaF}_2/\text{Si}(111)$. B: After electron irradiation. C: After Ge deposition at room temperature. D: 1 min, 490 °C anneal of C. E: 1 min 660 °C anneal of D.

would rather cover more Ge (high surface energy) than cover fluorine-terminated CaF_2 (low surface energy). An effective uniform thickness of 0.18 nm is equivalent to having 75% of the surface uncovered and the 3 ML originally deposited congealed into 12-ML thick islands on the other 25% of the surface. In two other growths, about 0.3 and 0.9 nm of Ge were deposited. After similar annealing sequences, the effective coverage has approximately the same temperature dependence (see Fig. 7), indicating that there is a similar amount of uncovered $\text{CaF}_2/\text{Si}(111)$ in all cases, with different amounts of Ge in the islands reflecting the different total coverages. As mentioned earlier, it is possible that islands begin to form already during the room-temperature deposition, and then further congeal into larger islands upon annealing.

A measure of the redistribution of the Ge over the surface which is independent of run-to-run fluctuations in collection efficiency²⁸ is the fraction of the intensity in the F 2s, Ge 3d, and Ca 3p which is due to Ge; this was obtained by fitting spectra such as those in the right panel of Fig. 5 with five Gaussians: F 2s, Ge 3d_{3/2}, Ge 3d_{5/2}, Ca 3p bulk, and Ca 3p interface. The results are shown in Fig. 7 for a variety of growths and annealing procedures.

2. Ge deposition on irradiated $\text{CaF}_2/\text{Si}(111)$

The tendency towards islanding and the sticking coefficient of Ge on CaF_2 are expected to be a strong function of the CaF_2 surface termination. To investigate this, we irradiated a portion of one $\text{CaF}_2/\text{Si}(111)$ sample with 3-keV electrons to remove the surface F layer. The

integrated beam current was chosen to be near the peak in efficiency for altering the morphology of thicker Ge films on $\text{CaF}_2/\text{Si}(111)$.¹⁴ Small changes in the fluoride valence-band structure measured with He I radiation were observed, but the large peak near the Fermi level reported by Karlsson *et al.*³³ was not, indicating that the irradiation may not have removed all of the surface fluorine. A layer of Ge was then deposited on the room-temperature substrate.

Photoemission spectra from the irradiated (right panel) and nonirradiated (7.5 mm away—left panel) portions of the sample are presented in Fig. 8. As can be seen there and in Fig. 7, the apparent thickness of Ge is different in the two cases, although the two spots were only 7.5 mm apart, and thus had the same exposure to the Ge source. The Ge layer deposited on the irradiated region has an apparent thickness twice that for the nonirradiated substrate, using the escape depths in Ref. 29. If islands do not dominate before the anneal, the most reasonable explanation is that the initial coefficient is much less for the nonirradiated surface than for the irradiated surface. This conclusion is the same if there is room-temperature island formation, since an increased sticking coefficient on the CaF_2 will cause more uniform growth and more deposition visible via photoemission. The Ge was evaporated slowly, taking 4 min to deposit the overlayer, which was approximately 2–3 ML thick on the nonirradiated surface and 5 ML thick on the nonirradiated region (as found from the decrease in the absolute F 2p and Si 2p intensities), assuming uniform coverage at room temperature. If instead we assume that all of the Ge sticks in both cases, then if the irradiated layer is uniform over the entire surface (5 ML thick as above), that same material must be redistributed to an average thickness of 8 ML over $\frac{5}{8}$ of the surface to explain the relative intensities.

Upon annealing the Ge overlayer, evidence for islanding can be seen in the spectra of Fig. 8. The Ge 3d intensity decreases relative to the Ca and F peaks. From comparison with growth at other thicknesses in Fig. 7, it can be seen that the evolution of the Ge: CaF_2 ratio with annealing is similar for the irradiated case as for the nonirradiated growth (growth 2) of similar thickness. This is a surprising result, since we expected the Ge/ CaF_2 interface to be more stable in the irradiated case and thus more resistant to balling up upon annealing. This indicates that the tendency for Ge to form bulk islands rather than thin films still dominates at these thicknesses of a few monolayers in the temperature range of 400–700 °C. The work of Kanemaru *et al.*¹⁴ involved Ge films 3–6 nm thick, where this may not have played as large a role. Also, the normal incidence electrons used in our experiment may not have been as efficient in removing fluorine as the grazing incidence electrons used in Ref. 14 due to the decreased interaction path in the interface region.

The change in the band offset at the $\text{CaF}_2/\text{Si}(111)$ interface which occurs upon Ge deposition is similar for both the irradiated and nonirradiated samples (see Fig. 6). The irradiated sample, however, does not recover upon annealing until a higher temperature than the nonirradiated, as can be seen in Fig. 6.

IV. SUMMARY AND CONCLUSIONS

We have investigated the role of lattice mismatch in controlling epitaxial semiconductor/insulator interface formation through the comparison of SrF₂/Si(111) and CaF₂/Si(111) growth. The valence-band offset and the principal local-bonding configuration at the interface are found to be the same for both interfaces, indicating that the chemical-bonding considerations dominate over the lattice mismatch in determining the local-bonding environment. Further studies must be done to determine the actual atomic structure of the interface and when the strain is relieved by defect formation. Our results are consistent with enough defects at the interface to account for a discommensurate interface.

The growth of a few monolayers of Ge on CaF₂/Si(111) is found to be enhanced by the irradiation of the CaF₂

film prior to the deposition of Ge. Both with and without irradiation, the valence-band offset at the buried interface is found to be reduced by about 1 eV, similar to the case of Au/CaF₂/Si(111).¹⁷ All films also show islanding behavior of the Ge upon annealing at temperatures of 400–700 °C.

ACKNOWLEDGMENTS

We are grateful for the skillful assistance of L. E. Swartz, R. D. Yingling, and J. D. Denlinger. Part of this work was performed at SSRL, which is supported by the Office of Basic Energy Sciences, U.S. Department of Energy (DOE). One of us (M.A.O.) was partially supported by National Science Foundation (NSF) Grant No. DMR-86-57623.

- ¹F. J. Himpsel, F. U. Hillebrecht, G. Hughes, J. L. Jordan, U. O. Karlsson, F. R. McFeely, J. F. Morar, and D. Rieger, *Appl. Phys. Lett.* **43**, 596 (1986).
- ²D. Reiger, F. J. Himpsel, U. O. Karlsson, F. R. McFeely, J. F. Morar, and J. A. Yarmoff, *Phys. Rev. B* **34**, 7295 (1986).
- ³M. A. Olmstead, R. I. G. Uhrberg, R. D. Bringans, and R. Z. Bachrach, *J. Vac. Sci. Technol. B* **4**, 1123 (1986).
- ⁴M. A. Olmstead, R. D. Bringans, R. I. G. Uhrberg, and R. Z. Bachrach, *Phys. Rev. B* **35**, 7526 (1987); in *Initial Stages of Epitaxial Growth*, Vol. 94 of *Materials Research Society Symposium Proceedings*, edited by R. Hull, J. M. Gibson, and D. A. Smith (MRS, Pittsburgh, 1987), p. 195; in *Proceedings of the 18th International Conference on the Physics of Semiconductors*, edited by O. Engström (World Scientific, Singapore, 1986), p. 255.
- ⁵F. J. Himpsel, U. O. Karlsson, J. F. Morar, D. Rieger, and J. A. Yarmoff, *Phys. Rev. Lett.* **56**, 1497 (1986).
- ⁶R. M. Tromp and M. C. Reuter, *Phys. Rev. Lett.* **61**, 1756 (1988).
- ⁷H. Ishiwara and T. Asano, *Appl. Phys. Lett.* **40**, 66 (1982).
- ⁸J. L. Batstone, J. M. Phillips, and E. C. Hunke, *Phys. Rev. Lett.* **60**, 1394 (1988); J. L. Batstone and J. M. Phillips, *ibid.* **61**, 2275 (1988).
- ⁹R. M. Tromp, F. K. LeGoues, W. Krakow, and L. J. Schowalter, *Phys. Rev. Lett.* **61**, 2274 (1988); R. M. Tromp, M. C. Reuter, F. K. LeGoues, and W. Krakow, *J. Vac. Sci. Technol. A* **7**, 1910 (1989).
- ¹⁰F. A. Ponce, G. B. Anderson, M. A. O'Keefe, and L. J. Schowalter, *J. Vac. Sci. Technol. B* **4**, 1121 (1986).
- ¹¹S. Satpathy and R. M. Martin, *Phys. Rev. B* **39**, 8494 (1989).
- ¹²J. M. Phillips, L. C. Feldman, J. M. Gibson, and M. L. McDonald, *J. Vac. Sci. Technol. B* **1**, 246 (1983); J. M. Gibson and J. M. Phillips, *Appl. Phys. Lett.* **43**, 828 (1983).
- ¹³Preliminary results were presented in M. A. Olmstead and R. D. Bringans, in *Heteroepitaxy on Silicon: Fundamentals, Structure, and Devices*, Vol. 116 of *Materials Research Society Symposium Proceedings*, edited by H. K. Choi, R. Hull, H. Ishiwara, and R. J. Nemanich (MRS, Pittsburgh, 1988), p. 419.
- ¹⁴S. Kanemaru, H. Ishiwara, and S. Furukawa, in *Initial Stages of Epitaxial Growth*, Vol. 94 of *Materials Research Society Symposium Proceedings*, edited by R. Hull, J. M. Gibson, and D. A. Smith (MRS, Pittsburgh, 1987), p. 71; *J. Appl. Phys.* **63**, 1060 (1988).
- ¹⁵H. C. Lee, T. Asano, H. Ishiwara, and S. Furukawa, *Jpn. J. Appl. Phys.* **27**, 1616 (1988).
- ¹⁶Preliminary results are presented in M. A. Olmstead and R. D. Bringans, in *Proceedings of the 19th International Conference on the Physics of Semiconductors*, edited by W. Zawadzki (Institute of Physics, Polish Academy of Sciences, Warsaw, 1988), p. 619.
- ¹⁷F. Xu, M. Vos, and J. H. Weaver, *Phys. Rev. B* **39**, 8008 (1989).
- ¹⁸B. K. Krusor, D. K. Biegelsen, J. Abelson, and R. D. Yingling, *J. Vac. Sci. Technol. B* **7**, 129 (1989).
- ¹⁹This sample had previously been utilized for CaF₂/Si(111) experiments, and sputtered and annealed to Si(111)(7×7). From the ratio of the photoemission cross sections given by J. J. Yeh and I. Lindau [*At. Data Nucl. Data Tables* **32**, 1 (1985)], if the Ca is at the interface and the interface component of the Sr 4*p* peak is a full monolayer, then the Ca is 5% of a monolayer. This does not affect the conclusions.
- ²⁰F. L. Batty, J. Liesegang, R. C. G. Leckey, and J. G. Jenkin, *Phys. Rev. B* **13**, 2646 (1976).
- ²¹J. P. Albert, C. Jouanin, and C. Gout, *Phys. Rev. B* **16**, 4619 (1977).
- ²²F. J. Himpsel, G. Hollinger, and R. A. Pollak, *Phys. Rev. B* **28**, 7014 (1983).
- ²³A. B. McLean and F. J. Himpsel, *Phys. Rev. B* **39**, 1457 (1989).
- ²⁴M. A. Olmstead, R. D. Bringans, R. I. G. Uhrberg, and R. Z. Bachrach, *Phys. Rev. B* **34**, 6401 (1986).
- ²⁵K. Nath and A. B. Anderson, *Phys. Rev. B* **38**, 8264 (1988).
- ²⁶J. D. Denlinger, M. A. Olmstead, E. Rotenberg, J. R. Patel, and E. Fontes (unpublished).
- ²⁷C. L. Strecker, W. E. Moddeman, and J. T. Grant, *J. Appl. Phys.* **52**, 6921 (1981).
- ²⁸It should be noted that small changes in the collection geometry can occur in the process of bringing the sample into the MBE chamber for growth and then returning to the mea-

- surement position, contributing to the uncertainty in the relative amplitudes of the spectra.
- ²⁹H. Gant and W. Mönch, *Surf. Sci.* **105**, 217 (1981).
- ³⁰H. Ishiwara and T. Asano, *J. Appl. Phys.* **55**, 3566 (1984).
- ³¹R. W. Grant, E. A. Kraut, S. P. Kowalczyk, and J. R. Waldrop, *J. Vac. Sci. Technol. B* **1**, 320 (1983); E. A. Kraut, R. W. Grant, J. R. Waldrop, and S. P. Kowalczyk, *Phys. Rev. B* **28**, 1965 (1983).
- ³²J. M. Reau, C. Lucat, G. Campet, J. Claverie, and J. Portier, *Electrochem. Acta* **22**, 761 (1977).
- ³³U. O. Karlsson, F. J. Himpsel, J. F. Morar, F. R. McFeely, D. Rieger, and J. A. Yarmoff, *Phys. Rev. Lett.* **57**, 1247 (1986).
- ³⁴R. W. G. Wyckoff, *Crystal Structures* (Interscience, New York, 1963), Vol. I.
- ³⁵Calculated from column 1 and Y. S. Touloukian, R. K. Kirby, R. E. Taylor, and P. D. Desai, *Thermal Expansion: Metallic Elements and Alloys*, Vol. 12 of *Thermophysical Properties of Matter* (IFI/Plenum, New York, 1975), and Y. S. Touloukian, R. K. Kirby, R. E. Taylor, and T. Y. R. Lee, *Thermal Expansion: Nonmetallic Solids*, Vol. 13 of *Thermophysical Properties of Matter* (IFI/Plenum, New York, 1977).
- ³⁶The measured value of the surface free energy varies with the measurement conditions and the equations used to relate the experimental results to the surface energy. These values were obtained under similar conditions and are thus appropriate for comparison.
- ³⁷J. J. Gilman, *J. Appl. Phys.* **31**, 2208 (1960).
- ³⁸R. J. Jaccodine, *J. Electrochem. Soc.* **110**, 524 (1963).
- ³⁹P. Kraatz and T. Zoltai, *J. Appl. Phys.* **45**, 4741 (1974).